

Fig. 1: SRF module to be installed at SRRC

Table II: Parameters relating to operating the SRF module of CESR III design at SRRC

Nominal machine energy	1.5 GeV
Revolution frequency	2.49827 MHz
Maximum beam current	< 500 mA
SR energy loss per turn	<164 keV
RF harmonic number	200
Beam power	< 82 kW
RF frequency	499.654 MHz
RF voltage	1.6 MV
Number of RF cavities	1
R/Q per cell ( $V^2/2Pc$ )	89/2
External Q	2.5E5
Cryogenic static load	< 30 W @4.5K

## 2 SRF MODULES

Inside the SRF module [2][3] is a 500MHz niobium radio frequency cavity operated at 4.5K in a liquid helium bath in a liquid nitrogen-shielded, vacuum insulated liquid helium vessel. The round beam tube (RBT) is attached to one side of the niobium cavity, and the flute beam tube (FBT) to the other side. The beam-line outside the cryostat of the SRF module consists of radio frequency higher order mode dampers connected to the longitudinal thermal transition pieces, a spool piece with a mechanical tuner [8] for cavity frequency adjustment, a sliding joint, and two tapers with synchrotron radiation masks on both ends that can be isolated by all-metal vacuum gate valves.

The RF power is delivered through a WR1800 air-filled waveguide, via a WR1800 H-bend elbow, to a Thomson's room temperature RF window situated underneath the cryostat. The RF window has a reduced height waveguide (18"x 4.5") on its vacuum side and is connected to a waveguide (17"x4") of step vacuum pumpout box. This pumpout box is then followed by a thermal transition waveguide (riser), a liquid nitrogen cooled double elbow, a cold helium gas cooled thermal transition waveguide (HEX), and a niobium waveguide inside the liquid helium vessel. A C-slot shaped coupling iris (tongue) [2] is employed in the end of the niobium waveguide to couple RF power into the cavity, with a nominal external quality

factor ( $Q_{ext}$ ) of 2.0E5 (including effects of step pumpout box.) Figure 1 depicts the layout of the SRF module to be installed at SRRC. Table II explicates the relevant parameters for operating the SRF module at SRRC. Yearly operating status of the SRF modules at CESR are found elsewhere [5][9][10][11][12][13].

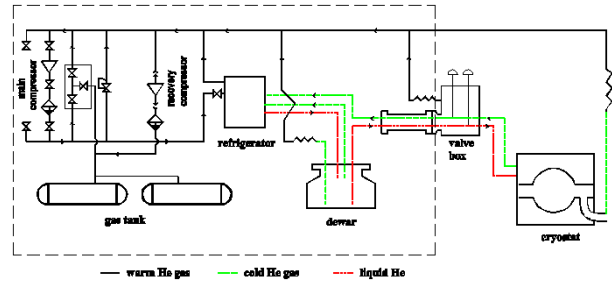


Fig. 2: Schematic layout of the cryogenic plant to support the SRF module at SRRC

Table III: Expected cryogenic loads of the SRF module (phase I) and of those with a superconducting harmonic module (phase II).

	Phase I	Phase II
SRF Cryostat under Normal Operation	80W+0.18g/s	2*(80W+0.18g/s)
2000 liters liquid He Dewar	30W (heater)	30W (heater)
Valve Box	10W	10W
LHe Multi-Channel Transfer Line	5W	15W
LHe Flexible Transfer Line	15W	30W
Connectors and control valves	20W	40W
Subtotal*	160W+0.18g/s	285W+0.36g/s

\*Cryogenic specification is the value multiplied by a safety factor of 1.5

## 3 CRYOGENIC PLANT

The cryogenic plant was specified to provide a minimum of 50/110 liter/hr of liquefying capacity and 240W/435W refrigerating capacity at 4.5K without/with pre-cooling of the refrigerator/liquefier by liquid nitrogen, respectively. The plant includes a screw-type helium compressor, an oil removal system, a gas management system, a turbo-expander type refrigerator/liquefier, two warm gaseous helium storage tanks (100m<sup>3</sup> each), one liquid helium dewar (2000 liters), one recovery compressor (4.56 m<sup>3</sup>/min) with its own oil removal, and helium transfer lines in between of these elements. The SRF module is attached to the cryogenic plant via a cryogenic valve box. Examining the helium inventory reveals that such a cryogenic plant can cool the SRF module at 40 K/hr.

The screw compressor is at a piping distance of 180 meters away from the storage ring and is installed on a separate concrete base that isolates the mechanical vibration. The SRF module is within a piping length of 6 meters to the refrigerator/liquefier and the main liquid helium dewar on a platform in the experimental hall, to avoid the necessity of phase separation due to cryogenic

loss during the long distance transfer of liquid helium. A combination of a screw compressor and a turbine refrigerator/liquefier was chosen as they can run continuously for a long time.

Cryogenic capacity was estimated according to the measured cryogenic loads of the SRF module of the CESR-III design at CESR [14], and included a safety factor of 1.5. A capacity reserved for a superconducting harmonic cavity to be implemented later is included. The cryogenic plant is loaded only by the SRF module during the first phase of operation. Therefore, a frequency driver for the main compressor will be employed to save energy and match the cryogenic load.

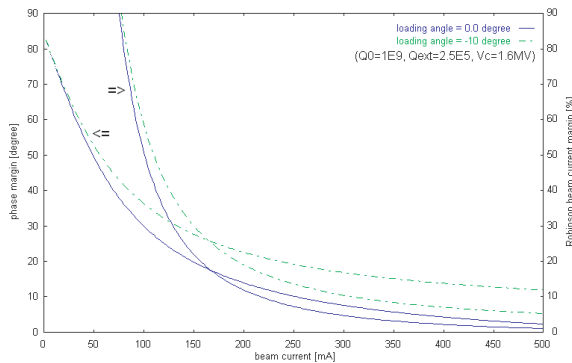


Fig. 3: Dependence of RF amplitude (threshold current) and phase stability margin to static Robinson instability on the beam current, with SRF module, at SRRC.

## 4 RF CONTROL AND MACHINE OPERATION

### 4.1 Static Robinson Instability

The storage ring at SRRC has a circumference of 120 meters, and is a small-circumference ring which prevents longitudinal coupled bunch instability driven by the fundamental mode of the accelerating cavity. However, the effects of heavy beam loading is still of great concern, which is conveniently characterized by the ratio of the beam-induced voltage at resonance ( $V_{br}$ ) to the cavity voltage ( $V_c$ ),  $Y=V_{br}/V_c$ . SRRC features the factor,  $Y$ , of 7 while operating the SRF module at a beam current of up to 500 mA. Operating the RF system with insufficient stable margin to static Robinson instability may degrade the stability of synchrotron light. Detuning the cavity to a non-zero loading angle (e.g.  $-10^\circ$ ) increases the amplitude and the phase stable margin, as illustrated in Fig. 3, and compensating with increased RF reverse power. An increase in reverse power tends to reduce the resonance level and to broaden the resonance band of multipacting [15], further causing difficulty in processing the multipacting. Implementing direct feedback is another effective means of increasing the margin, but without the cost of extra reverse power. Beam testing of the direct feedback using the existing room temperature accelerating cavities at SRRC is now being undertaken.

### 4.2 Coupled bunch Instabilities

Performance of the light source facility at SRRC is currently limited by the longitudinal coupled bunch instabilities primarily driven by the higher order modes of the Doris cavities operated at room temperature. Amplitude modulation of the RF gap voltage around the double of the synchrotron oscillation frequency is applied routinely, with fine tuning of second cavity plunger tuners, by careful selection and stabilization of cavity cooling water temperatures. A marked increase of the instability threshold is expected to follow the installation of the SRF module. The ultimate suppression of longitudinal coupled bunch instabilities can only rely on a broadband feedback mechanism, due to unavoidable residual impedance of the rest ring components. The digital longitudinal feedback is currently being developed to satisfy the synchrotron light specification at high beam current. Moreover, transverse coupled bunch instabilities become much stronger after the longitudinal coupled bunch instabilities have been suppressed. The transverse feedback system is ready.

### 4.3 Beam lifetime

The synchrotron light users benefit from a long beam lifetime. Nevertheless, the lifetime of a low emittance storage ring operated at low to medium energy is commonly insufficient due to large-angle intrabeam (Touschek) scattering of the electrons within bunches. This shortage becomes important for operating the storage ring at SRRC at higher beam current. Increasing the total RF gap voltage initially helps to avoid electron loss due to Touschek scattering by increasing the energy acceptance, but the Touschek life time eventually compressed by bunch length shortening at a higher gap voltage. The SRF module was therefore optimized to operate at 5.33 MV/m or a 1.6 MV gap voltage to maximize the Touschek lifetime [16]. Implementing harmonic cavities to extend the bunch length is principally effective in increasing the Touschek lifetime for a low energy machine and has been employed for some of third generation light source facilities. However, transient beam loading due to a finite bunch gap, used for ion-cleaning may significantly constrain the lifetime improvement [17]. The mechanism governing behind must be carefully examined by particle tracking code.

### 4.4 RF heating at high beam current

After the SRF module is installed at SRRC, the machine will be first commissioned at 200mA and the accumulated current is expected to increase rapidly after carefully examining the RF heating on the vacuum chamber as well as the radiation dose outside the existing radiation shielding designed for operation at 200mA. Modification of vacuum chambers, front ends, and beam lines may be required for improved cooling.

## 5 LONG TERM PERFORMANCE

The first SRF module was installed at CESR in September, 1997. Since then, five SRF modules have been fabricated and four of them are routinely operated at a maximum RF power, routinely delivering over 200kW each. Operating SRF modules at CESR offers invaluable lessons in performance and parameter optimization. Some operational concerns involve previous experiences of operating the SRF module at CESR, to develop a strategy for smooth operation at SRRC, as discussed below.

### 5.1 Hydrogen condensation

The long term performance of the SRF module is strongly influenced by the condensation of the residual gases on the cold surfaces of the module, i.e., cavity cell and RF coupler. The cold surface of the SRF module serves as a huge cryogenic pump capable of condensing the residual gases. Among them, hydrogen is most troublesome. Adsorbed gas evolution while warming up of the CESR SRF modules has been studied [18]. Results showed that the RF ceramic window is one of the most likely gas sources in the SRF module.

The cryogenic pumping may saturate after few months of continued operation, due to a decrease in the hydrogen sticking coefficients following condensation of a few mono-layers of hydrogen on the cold surface [18]. The vacuum gradually degrades in time and the electron beam may finally trip frequently owing to a vacuum burst, following the evacuation of condensed gas by RF heating on the cold surface. Such a phenomenon is associated with releasing condensed hydrogen from the cold surface of the SRF module at CESR [11]. Although the initial performance can be restored by warming the SRF modules to release the adsorbates, scheduled warm-up of the SRF module may still be harmful for efficiently operating the light source facility, if frequent thermal cycles are required for stable operation.

Following Cornell, the HEX section is improved by modifying the gas helium cooling channels and reducing the RF heat loss on the inner waveguide surface by copper plating to a thickness of 15 $\mu$ . This thickness is much greater than the corresponding skin depth foreseen for the SRF modules operated at 500MHz. In addition to the two 500 lit/sec ion pumps on the tapers, two 150 lit/sec ion pumps will be installed on the pumpout box of the RF window to improve the pumping speed even though the speed remains much lower than that of the cryogenic pump of the waveguide cold surface, 600l/s [19]. The use of NEG pumps to increase the hydrogen pumping speed is being studied.

Baking the RF windows and the other waveguide components (except niobium cavity) for a long period prior to the assembly of the SRF module has been requested to reduce the gas loads. The RF windows will be conditioned off-line up to 200 kW CW RF power (safety factor of two) in traveling wave mode and 50 kW CW RF power in standing wave mode, with the ceramic window positioned at various phases, over a conditioning

time long enough (2 hours) to reach thermal stability. These actions will help to minimize the in-situ processing time and reduce the gas loads on the ceramic.

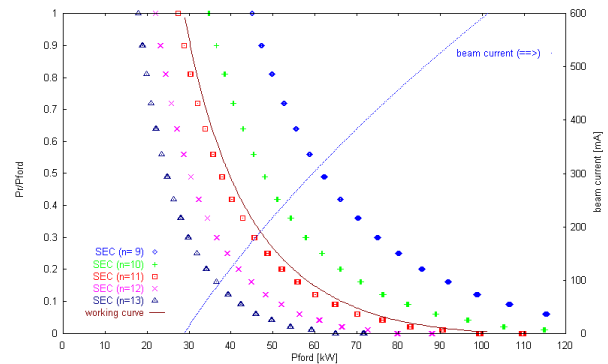


Fig. 4: Multipacting susceptibility of a reduced height waveguide (17"x4") while operating the SRF module at a beam current of up to 500mA at SRRC, according to the analytical approach. These multipacting lines with orders from 9 to 13 are processable according to CESR's experience.

### 5.2 Multipacting

Gas condensation may enhance field emission and multipacting. Effects on field emission may not be of crucial in our application, because the SRF module will operate at a medium gradient, 5.33 MV/m. Nevertheless, multipacting, due to resonant electron bombardment, depends strongly on the secondary emission coefficient (SEC) of the material surface. SEC might be enhanced by hydrogen condensation on the cold surface of the niobium waveguide. Consequently, more multipacting bands become active to cause RF trips. This kind of vacuum trip was first observed at CESR with a beam power of 90 kW [11], as a remarkable multipacting barrier associated with multipacting in the RF coupler region because of its repeatability.

The dependence of multipacting resonance on the forward power is analytically obtainable [20][21] by ignoring the trajectory migration of multipacting electrons driven by the transverse magnetic field component. Figure 4 presents the working curve of the SRF module at SRRC for forward power up to 600mA. Displayed are also the multipacting resonance lines with orders 9, 10, 11, 12, 13, and the corresponding operating beam current.

### 5.3 Vacuum tightness after thermal cycles

Vacuum leakage after several thermal cycles of the cryostat is also of great concern. Verification of vacuum tightness will be examined during high power horizontal test of the SRF modules at CESR in 2002, and repeated at SRRC after shipment overseas. Vacuum tightness up to  $2 \cdot 10^{-10}$  mbar l/sec from the niobium cavity to ambient and to the helium tank is specified, and up to  $2 \cdot 10^{-8}$  mbar l/sec from the helium tank to the isolation vacuum and from the isolation vacuum to ambient.

#### 5.4 Surface contamination and vacuum accidents

A highly criticized issue in using superconducting RF modules in a light source facility, rather than in using a room temperature cavity is the high risk of surface contamination following a vacuum accident. At SRRC, tens of beam lines have been implemented for various experimental stations, along the storage ring with a circumference of 120 meters. Vacuum gate valves will be implemented in both ends of the SRF module's beam lines, triggered by sophisticated interlock chain, to prevent air exposure of cold surface following a vacuum accident at the beam line's front ends. SRF performance is expected to be recoverable after high power RF processing.

### 6 PERSPECTIVE

Intensive SRF training has been undertaken, thanks to strong technical support from the SRF laboratory at Cornell. The training items included the chemical processing of niobium cavities, vertical testing of niobium cavity, cryostat assembly, horizontal testing, RF window conditioning, SRF module installation, commissioning, routine warm-up and cool-down, RF processing, and operation coordination between the SRF module and cryogenic plant. In-house training continued for duplicating the CESR designed quench detector, exercising the vacuum seal with indium as well as cold shock of the waveguide flange and flute flange. The coming year will emphasize more attention paid to mastering the routine operation of the SRF module. The skills required for minimizing the machine trips must be enhanced.

### 7 ACKNOWLEDGMENTS

The authors are grateful to Prof. H. Padamsee for his continuous support and encouragement. S. Belomestnykh, J. Knobloch, R.L. Geng, J. Sears, P. Quigley, J. Reilly, R. Ehrlich (Cornell University), and J. Mulholland (ACT) are especially appreciated for their consistent technical support. M. Pekeler (ACCEL) is also commended for his many valuable discussions and constructive comments.

### 8 REFERENCES

[1] R. Sah et al., "Operations and upgrades at SRRC," *Proc. of the 7<sup>th</sup> EPAC*, 2000, pp.684-686.  
[2] H. Padamsee, et al., "Design challenges for high current storage rings," *Part. Accel.*, 40, pp. 17-41 (1992).  
[3] S. Belomestnykh et al., "Running CESR at high luminosity and beam current with superconducting RF system," *Proc. of the 5<sup>th</sup> EPAC*, 1996, pp.2100-2102.  
[4] H. Padamsee, "Review of experience with HOM damped cavities," *Proc. of the 8<sup>th</sup> EPAC*, 1998, pp.184-188.

[5] S. Belomestnykh et al., "Running CESR at high luminosity and beam current with superconducting RF system," *Proc. of the 7<sup>th</sup> EPAC*, 2000, pp.2025-2027.  
[6] H. Vogel et al., "Superconducting accelerator modules for the Taiwan Light Source," *Proc. of the 7<sup>th</sup> EPAC*, 2000, pp.711-713.  
[7] M. Pekeler et al., "Latest results from the production of 500 MHz SRF modules for light sources and CESR upgrade," this proceeding.  
[8] E. Nordberg et al., "Cryostat for a beam test with the CESR-B cavity," *Proc. 1993 PAC*, pp. 995-997.  
[9] S. Belomestnykh et al., "Development of superconducting RF for CESR," *Proc. 1997 PAC*, pp.3075-3077.  
[10] S. Belomestnykh et al., "The high luminosity performance of CESR with the new generation superconducting cavity," *Proc. 1999 PAC*, pp.272-276.  
[11] S. Belomestnykh et al., "Commissioning of the superconducting RF cavities for the CESR luminosity upgrade," *Proc. 1999 PAC*, pp.980-982.  
[12] S. Belomestnykh et al., "Operating experience with superconducting RF at CESR and overview of other SRF related activities at Cornell university," *9<sup>th</sup> Workshop on RF Superconducting*, 1999.  
[13] S. Belomestnykh et al., "Superconducting RF system upgrade for short bunch operation of CESR," *Proc. 2001 PAC*, pp.272-276.  
[14] E. Chojnacki and J. Sears, "Superconducting RF cavities and cryogenics for the CESR III upgrade," *9<sup>th</sup> Workshop on RF Superconducting*, 1999.  
[15] R.L. Geng and H.S. Padamsee, "Exploring multipacting characteristics of a rectangular waveguide," *Proc. 1999 PAC*, pp.429-431.  
[16] G.H. Luo et al., "The superconducting rf cavity and 500 mA beam current upgrade project at Taiwan Light Source," *Proc. of the 7<sup>th</sup> EPAC*, 2000, pp.654-656.  
[17] J. Byrd, "Transient beam loading in the ALS harmonic system," *Proc. of the 7<sup>th</sup> EPAC*, 2000, pp.1113-1115.  
[18] R.L. Geng et al., "Condensation/adsorption and evacuation of residual gases in the SRF system for the CESR luminosity upgrade," *Proc. PAC 1999*, p983-985.  
[19] R.L. Geng and P. Barnes, "Pumping speed near the RF window of the CESR SRF cavity," LNS Report, SRF-980227-02, Cornell Univ.  
[20] V. Shemelin, "Multipactor discharge in a rectangular waveguide with regard to normal and tangential velocity components of secondary electrons," LNS Report, SRF-010322-03, Cornell Univ..  
[21] R.L. Geng et al., "Multipacting in a rectangular waveguide," *Proc. PAC 2001*.